

A rational approximation method for solving acoustic nonlinear eigenvalue problems

Mohamed El-Guide^{a,*}, Agnieszka Międlar^{b,2} and Yousef Saad^{c,3}

^aMohammed VI Polytechnic University, The Faculty of Governance, Economic and Social Sciences, Green City, Morocco and University of Minnesota, Department of Computer Science & Engineering, 4-192 Keller Hall, 200 Union Street SE, Minneapolis, MN 55455, USA

^bUniversity of Kansas, Department of Mathematics, 405 Snow Hall, 1460 Jayhawk Blvd. Lawrence, KS 66045-7594, USA

^cUniversity of Minnesota, Department of Computer Science & Engineering, 4-192 Keller Hall, 200 Union Street SE, Minneapolis, MN 55455, USA

ARTICLE INFO

Keywords:

nonlinear eigenvalue problem, boundary element method, rational approximation, Cauchy integral formula

ABSTRACT

We present two approximation methods for computing eigenfrequencies and eigenmodes of large-scale nonlinear eigenvalue problems resulting from boundary element method (BEM) solutions of some types of acoustic eigenvalue problems in three-dimensional space. The main idea of the first method is to approximate the resulting boundary element matrix within a contour in the complex plane by a high accuracy rational approximation using the Cauchy integral formula. The second method is based on the Chebyshev interpolation within real intervals. A Rayleigh-Ritz procedure, which is suitable for parallelization is developed for both the Cauchy and the Chebyshev approximation methods when dealing with large-scale practical applications. The performance of the proposed methods is illustrated with a variety of benchmark examples and large-scale industrial applications with degrees of freedom varying from several hundred up to around two million.

1. Background and Introduction

The Boundary Element Method (BEM) is a powerful approach developed to solve integral equations [1]. The application of the BEM method has gained popularity in many branches of science and engineering over the past few years, e.g., in elasticity, ground and water flow, wave propagation and in electromagnetic problems [2]. The most commonly used approaches for numerically solving PDEs are the Finite Difference Method (FDM) and the Finite Element Method (FEM). A standard finite difference method is suitable when dealing with simple domains (e.g. rectangular grids), while the finite element method can handle more complex domains. However, the computational work involved to numerically discretize the full domain (generate meshes) and solve the resulting discretized problem becomes excessive when dealing with complicated domains in higher dimensions, i.e., $d \geq 3$. This is where BEM becomes appealing as it allows to significantly reduce the overall computational complexity of the solution process. Instead of solving a problem for the partial differential operator defined on the whole domain Ω , the boundary element method uses an associated boundary integral equation reducing the domain of the problem to the boundary $\partial\Omega$. This comes at a cost since the matrix problem to solve in the approximation becomes dense.


In the following, we are interested in the efficient solution of nonlinear eigenvalue problems (NLEVPs) resulting from the boundary element (BE) discretization of acoustic


problems. Although a finite element discretization of the problem yields a generalized (linear) eigenvalue problem, it requires a discretization of the whole domain Ω which is not always feasible, e.g., if the domain is unbounded. Though the topic of NLEVPs built upon the boundary element method (BEM) has been around for a number of years, the lack of efficient eigensolvers has delayed a full exploration of BE-based approaches. Recently, eigenvalue solvers based on contour integrals were developed and this made BEM an attractive alternative to the usual contenders when solving challenging nonlinear eigenvalue problems [3, 4, 5]. Contour based methods have the ability to solve NLEVPs when the eigenvalues of interest lie inside a given closed contour in the complex plane using rational or polynomial approximation [6, 7, 8, 9, 10]. Despite these efforts, solving NLEVPs is still a computationally intensive task. Assembling interpolation matrices and solving linear systems in the BE framework are already very expensive due to the unstructured, dense and complex nature of the resulting matrices. For example, the Chebyshev interpolation of the BE formulation of the large-scale acoustic problem discussed in [6] results in a generalized eigenvalue problem which cannot be easily handled with the state-of-the-art linear solvers. Another drawback of this method is that the quality of the approximations quickly deteriorates when dealing with complex eigenvalues.

It is the purpose of this paper to overcome the aforementioned difficulties and develop eigensolvers suitable for calculations of eigenvalues of NLEVPs arbitrarily located in the complex plane. The paper illustrates the performance of the proposed method with a problem that arises in the modal analysis of large-scale acoustic problems. Here we follow the notation of [11, 12].

Consider the three-dimensional (3D) acoustic Helmholtz

*Corresponding author

 mohamed.elguide@um6p.ma (M. El-Guide); amiedlar@ku.edu (A. Międlar); saad@umn.edu (Y. Saad)

 <http://miedlar.faculty.ku.edu/> (A. Międlar); <https://www-users.cs.umn.edu/~saad/> (Y. Saad)

ORCID(s):

¹Work supported by NSF grant 1812927.

²Work supported by NSF grant 1812695.

equation

$$\Delta p(x) + \lambda^2 p(x) = 0, \quad x \in \Omega \subset \mathbb{R}^3, \quad (1)$$

where Δ is the Laplace operator, $p(x)$ is the sound pressure at point x , $\lambda = \omega/c$ is the wave number with the circular frequency ω and the speed of sound c through the fluid medium.

Equation (1) is subject to a homogeneous condition on its boundary $\partial\Omega$ of the form

$$a(x)p(x) + b(x)\frac{\partial p(x)}{\partial n} = 0, \quad x \in \partial\Omega, \quad (2)$$

where $\frac{\partial}{\partial n}$ denotes the outward normal to the boundary at point x . Using BEM yields the following Helmholtz integral equation [13]

$$C(x)p(x) + \int_{\partial\Omega} \frac{\partial g(x, y)}{\partial n_y} p(y) dy = \int_{\partial\Omega} g(x, y) \frac{\partial p(y)}{\partial n_y} dy, \quad (3)$$

where C denotes the solid angle at point x [13], n_y the surface unit normal vector at point y and $g(\cdot, \cdot)$ the free-space Green's function [14, 15, 11],

$$g(x, y) = \frac{e^{i\lambda\|x-y\|}}{\|x-y\|} \quad (\text{in the 3D case}). \quad (4)$$

The continuous Helmholtz integral equation (3) can be discretized to form the following discrete problem from which the boundary node pressure values p can be determined,

$$H(\lambda)u = G(\lambda)q, \quad (5)$$

where H and G are discretization of the left and right side of the Helmholtz integral equation (3), respectively; u and q are vector collections of the nodal pressure p and its normal derivative, respectively [13]. Note that (2) generally appears in the following Robin boundary condition form

$$\frac{\partial p(x)}{\partial n} = -i \frac{\rho_0 \omega}{Z(x)} p(x), \quad (6)$$

where ρ_0 is the density of the fluid and Z is the acoustic impedance. In this case, the boundary element discretization of (6) can be expressed as

$$q(\lambda) = B(\lambda)u, \quad (7)$$

where B is a diagonal matrix consists of the nodal values of $-i \frac{\rho_0 \omega}{Z(x)}$. The continuous Helmholtz integral equation (3) can be then discretized to form the following discrete problem

$$T(\lambda)u = 0, \quad T(\lambda) := H(\lambda) - G(\lambda)B(\lambda). \quad (8)$$

Here, $T(\lambda)$ is a matrix function that is nonlinear in λ and holomorphic since the free-space Green's functions are holomorphic functions of λ . Obviously, equation (8) is a NLEVP and the objective of this paper is to develop methods for finding all eigenvalues λ , satisfying (8), that are located inside a certain region of the complex plane enclosed by the contour Γ .

2. Rational and Chebyshev approximation methods for NLEVPs

The first method we consider is adapted from [16] and it is based on the Cauchy integral formula. Given a Jordan curve Γ that surrounds the eigenvalues of interest, we express the matrix function $T(\lambda)$ as follows:

$$T(\lambda) = \frac{1}{2i\pi} \int_{\Gamma} \frac{T(z)}{z-\lambda} dz. \quad (9)$$

By replacing both occurrences of $T(\cdot)$ in (9) by $T_{ij}(\cdot)$, one can see that the above expression is equivalent to expressing each individual entry $T_{ij}(\lambda)$ of $T(\lambda)$ by the Cauchy integral formula. Equality (9) is valid for z inside the contour Γ and the only requirement is that $T(\lambda)$ be analytic inside Γ . As is classically done [17] we use a numerical quadrature formula to obtain the following Cauchy integral approximation $\tilde{T}(\lambda)$ of $T(\lambda)$

$$\tilde{T}(\lambda) \approx \sum_{i=0}^m \frac{\omega_i T(\sigma_i)}{\lambda - \sigma_i}, \quad (10)$$

where the σ_i 's are quadrature points located on the contour Γ and the ω_i 's the corresponding quadrature weights. Setting $B_i = \omega_i T(\sigma_i)$, equation (10) can be rewritten as

$$\tilde{T}(\lambda) = \frac{B_0}{\lambda - \sigma_0} + \frac{B_1}{\lambda - \sigma_1} + \dots + \frac{B_m}{\lambda - \sigma_m}, \quad (11)$$

$$= B_0 f_0(\lambda) + B_1 f_1(\lambda) + \dots + B_m f_m(\lambda), \quad (12)$$

with $f_i(\lambda) = \frac{1}{\lambda - \sigma_i}$, $i = 0, \dots, m$. For a given vector u we now define

$$v_i := f_i(\lambda)u, \quad \text{for } i = 0, \dots, m.$$

Then the approximate nonlinear eigenvalue problem $\tilde{T}(\lambda)u = 0$ yields

$$\tilde{T}(\lambda)u = B_0 v_0 + B_1 v_1 + \dots + B_m v_m = 0. \quad (13)$$

Chebyshev interpolation of order m can also be used to obtain the same form as (12) of the approximation of the matrix-valued function $T(z)$. In this method, proposed in [6], the function $T(\lambda)$ is expanded using a degree m Chebyshev polynomial expansion of the form [18]:

$$\tilde{T}(\lambda) = B_0 \tau_0(\lambda) + B_1 \tau_1(\lambda) + \dots + B_m \tau_m(\lambda), \quad (14)$$

where B_i and $\tau_i(z)$ are coefficient matrices and Chebyshev basis functions, respectively. The corresponding nonlinear eigenvalue problem is of the same form as (13) with the vectors v_i now defined by $v_i = \tau_i(z)u$.

The problem (13) for the Cauchy interpolation, and its Chebyshev interpolation counterpart, can be reformulated as a generalized linear eigenvalue problem:

$$Aw = \lambda Mw. \quad (15)$$

For the Cauchy rational approximation we have:

$$\mathcal{A} = \begin{bmatrix} \sigma_0 I & & & I \\ & \sigma_1 I & & I \\ & & \ddots & \vdots \\ -B_0 & -B_1 & \cdots & \sigma_m I \\ & & & -B_m & 0 \end{bmatrix},$$

$$\mathcal{M} = \begin{bmatrix} I & & & \\ & I & & \\ & & \ddots & \\ & & & \ddots \\ & & & & 0 \end{bmatrix}, \quad (16)$$

and $w = [v_0^T, v_1^T, \dots, v_m^T, u^T]^T$ whereas for the Chebyshev interpolation

$$\mathcal{A} = \begin{bmatrix} 0 & I & & & & \\ I & 0 & I & & & \\ & \ddots & \ddots & \ddots & & \\ -B_0 & \cdots & -B_{m-3} & C_{m-2} & -B_{m-1} & \\ & & & & & I \end{bmatrix},$$

$$\mathcal{M} = 2 \begin{bmatrix} \frac{1}{2} I & & & & & \\ & I & & & & \\ & & \ddots & & & \\ & & & I & & \\ & & & & & B_m \end{bmatrix}, \quad (17)$$

where $C_{m-2} \equiv B_m - B_{m-2}$ and $w = [u^T, v_1^T, \dots, v_{m-1}^T, v_m^T]^T$.

With regards to the rational approximation described above, we note that an alternative that has been used with some success in the literature is the Barycentric approximation formula [8]. However, our tests with this technique showed no significant improvement in our context over the simple Cauchy formula used above. Note that it is also possible to exploit other polynomials, using different classes of orthogonal polynomials but we will restrict our attention to Chebyshev polynomials of the first kind. Finally note that Chebyshev approximation works best for eigenvalues located in an interval while the Cauchy rational approximation is suitable for general complex spectra.

3. Rayleigh-Ritz procedure for BEM eigenvalue problem

Let U be a basis of dimension ν of a subspace that contains good approximations of the eigenvectors of the NLEVP problem (5). Then, it is possible to apply a Rayleigh-Ritz procedure to (5) to obtain approximate eigenpairs. The approximate eigenvector will be of the form $u = Uy$ with $y \in \mathbb{C}^\nu$. Then expressing that $T(z)u$ is orthogonal to the range of U yields the projected problem $U^H T_U(z)u = 0$ or,

$$\widehat{B}_0 f_0(z)y + \widehat{B}_1 f_1(z)y + \dots + \widehat{B}_m f_m(z)y = 0, \quad (18)$$

where $\widehat{B}_i = U^H B_i U$. We will denote $T_U(z)$ the projected operator, namely,

$$T_U(z) = \widehat{B}_0 f_0(z) + \widehat{B}_1 f_1(z) + \dots + \widehat{B}_m f_m(z). \quad (19)$$

Then, applying the same procedure as before to the projected problem we see that (18) becomes:

$$\widehat{B}_0 \widehat{v}_0 + \widehat{B}_1 \widehat{v}_1 + \dots + \widehat{B}_m \widehat{v}_m = 0, \quad (20)$$

with $\widehat{v}_i = \frac{y}{z - \sigma_i}$ in the case of rational approximation and $\widehat{v}_i = \tau_i(z)y$ when a Rayleigh-Ritz procedure is applied to the Chebyshev interpolation.

3.1. Solution of the reduced NLEVP

Analogously to what was discussed in Section 2, the problem (20) for the Cauchy rational approximation, as well as its Chebyshev interpolation counterpart, can be written down in a block form (15), but now of much smaller dimension. The projected nonlinear problem (20) yields the following linearized problem

$$\mathcal{A}w = \lambda \mathcal{M}w, \quad (21)$$

with $w = [\widehat{v}_0^T, \widehat{v}_1^T, \dots, \widehat{v}_m^T, y^T]^T$ and

$$\mathcal{A} = \begin{bmatrix} \sigma_1 I & & & I \\ & \sigma_2 I & & I \\ & & \ddots & \vdots \\ -\widehat{B}_1 & -\widehat{B}_2 & \cdots & \sigma_m I \\ & & & -\widehat{B}_m & 0 \end{bmatrix},$$

$$\mathcal{M} = \begin{bmatrix} I & & & \\ & I & & \\ & & \ddots & \\ & & & \ddots \\ & & & & 0 \end{bmatrix} \quad (22)$$

for the Cauchy rational approximation, and

$$w = [y^T, \widehat{v}_1^T, \dots, \widehat{v}_{m-1}^T, \widehat{v}_m^T]^T,$$

$$\mathcal{A} = \begin{bmatrix} 0 & I & & & & \\ I & 0 & I & & & \\ & \ddots & \ddots & \ddots & & \\ -\widehat{B}_0 & \cdots & -\widehat{B}_{m-3} & \widehat{C}_{m-2} & -\widehat{B}_{m-1} & \\ & & & & & I \end{bmatrix},$$

$$\mathcal{M} = \begin{bmatrix} I & & & & & \\ & 2I & & & & \\ & & \ddots & & & \\ & & & 2I & & \\ & & & & & 2\widehat{B}_m \end{bmatrix} \quad (23)$$

for the Chebyshev interpolation, where $\widehat{C}_{m-2} = \widehat{B}_m - \widehat{B}_{m-2}$. If ν is fairly small, the problem (21) can be solved directly, i.e., using standard dense packages. When ν is larger, the problem must be handled differently by some iterative procedure. Since for BEM problems the matrices B_i are generally complex, dense and unstructured, solving these linear eigenvalue problems can be computationally expensive. Therefore, it may be advantageous to rely on subspace iteration or an Arnoldi-type method to solve (21).

Note that for both the Cauchy rational approximation and the Chebyshev interpolation method, the matrices \mathcal{A} and \mathcal{M} don't have to be formed explicitly. If the partial solution of the problem (21) are of interest, effective methods such as the Implicitly Restarted Arnoldi method can be used to find a few of the extreme eigenvalues. Unfortunately, these methods become expensive when the eigenvalues of interest are deep inside the spectrum.

Alternatively, we can solve the interior eigenvalue problem with the help of the shift-and-invert technique, which replaces the solution of the generalized eigenvalue problem (21) by the following problem

$$\mathcal{H}w = \frac{1}{\lambda - \sigma}w, \quad \mathcal{H} := (\mathcal{A} - \sigma\mathcal{M})^{-1}\mathcal{M}. \quad (24)$$

Using the Arnoldi or the subspace iteration method to extract extreme eigenvalues of (24) will result in approximations of the eigenvalues of (21) closest to σ . Again, the matrix \mathcal{H} need not be formed explicitly to compute the matrix-vector product $y = \mathcal{H}x$. Instead, we can use a simple *LU* factorization that takes advantage of the sparsity of \mathcal{A} and \mathcal{M} . First, note that the matrix $(\mathcal{A} - \sigma\mathcal{M})$ is of the form

$$\begin{bmatrix} D & F \\ B & C \end{bmatrix}. \quad (25)$$

By exploiting the sparsity of the matrices D and F , we can easily form the following *LU* factorization

$$L = \begin{bmatrix} I & 0 \\ BD^{-1} & I \end{bmatrix}, \quad U = \begin{bmatrix} D & F \\ 0 & S \end{bmatrix}, \quad (26)$$

where $S = C - BD^{-1}F$ is known as the *Schur complement* of the block C . With the use of matrix S , we can use the Arnoldi algorithm on vectors of shorter length. Solving the shifted and inverted problem (24) with Arnoldi algorithm requires solving linear systems of the form

$$\begin{bmatrix} D & F \\ B & C \end{bmatrix} \begin{bmatrix} x \\ y \end{bmatrix} = \begin{bmatrix} a \\ b \end{bmatrix}. \quad (27)$$

Using the Schur complement S , y can be easily obtained by solving $Sy = b - BD^{-1}a$. Note that D is a diagonal matrix and F is a block of identity matrices. Once y is computed, x can be recovered by solving the trivial system $Dx = a - Fy$.

3.2. Construction of the subspace of approximants

We begin this section by noting that the Arnoldi-type or subspace iteration methods discussed in the previous section can be applied to a linear eigenvalue problem $\mathcal{A}w = \lambda\mathcal{M}w$ obtained directly from (13). However, proceeding in this way would require either solving linear eigenvalue problems of size $mn + n$ when using Arnoldi-type methods, or storing vectors of length $mn + n$ in the subspace iteration method, and this can be computationally expensive when m is large. Therefore, it is important to develop a technique that allows to work with subspaces of smaller dimensions that requires storing shorter vectors. A procedure of this type,

which works with subspaces of dimension m is presented next.

Let us first consider a large linear eigenproblem of the form (15) obtained from (13) without a projection. To introduce the approach that works with vectors of dimension n , we first point out that for an approximate eigenpair (λ, u) , u is the bottom (resp. top part) of an approximate eigenvector w of the large linear eigenvalue problem (15) associated with (12) for the Cauchy rational approximation, (resp. (14) for the Chebyshev interpolation). Let $W^{(0)}$ be a random initial set of ν basis vectors of a certain subspace, where each of the ν columns is of the form ³ $w = [v; u]$ (resp. $w = [u; v]$) for the splitting associated with the Cauchy rational approximation (resp. Chebyshev interpolation). Next, in order to make these initial random vectors close to the eigenvectors of interest, we apply q steps of the inverse power method with matrix \mathcal{H} in (24) to each column of $W^{(0)}$ separately. A subspace of dimension n that approximates the eigenvectors of (13) is then obtained from the bottom parts (resp. top parts) of the processed columns for the Cauchy rational approximation (rep. Chebyshev interpolation). Although this process involves the column vectors of $W^{(0)}$, only vectors of length n need to be saved and the iterates v can be discarded. The accuracy of the extracted eigenpairs obtained from applying a Rayleigh-Ritz projection can be further refined by updating U in a process that takes advantage of the structure of the approximate eigenvectors. Let (λ, u) be an approximate eigenpair of (13) obtained from applying a Rayleigh-Ritz projection using U . The new redefined vector w for each interpolation method is discussed next. For the Cauchy rational approximation, the vector $v = [v_1; v_2; \dots; v_m]^T$ (the top part of vector w), is obtained by setting $v_i = \frac{u}{\lambda - \sigma_i}$, whereas for the Chebyshev interpolation (the bottom part of vector w) it is defined by setting $v_i = \tau_i(\lambda)u$.

3.3. The inverse power method

The straightforward linearizations (16) of the Cauchy rational approximation and (17) of the Chebyshev interpolation, discussed in Section 2, are high dimensional problems and they become computationally demanding as the order m of the approximations grows. The Rayleigh-Ritz approach discussed above is inexpensive even if m is large. The biggest computational task of the presented Rayleigh-Ritz projection lies in performing q steps of the inverse power method with the matrix $(\mathcal{A} - \sigma\mathcal{M})^{-1}\mathcal{M}$. It is the purpose of the following discussion to show how each step of the inverse power method can be carried out inexpensively. For simplicity, we will assume that the shift σ is the center of the unit circle (resp. interval $[-1, 1]$) for the Cauchy rational approximation (resp. Chebyshev interpolation). This is a natural choice, since any circle in the complex plane can be scaled to the unit circle and any real interval $[a, b]$ can be scaled to the interval $[-1, 1]$. Throughout this discussion, the superscript j will correspond to the iteration number, while the subscript i will correspond to the blocks of the vectors $v^{(j)}$.

³Here we use Matlab notation: $[v; u]$ is a vector that stacks v on top of u .

We begin by discussing the inverse power method for the Cauchy rational approximation.

Inverse power iteration for the Cauchy rational approximation. For the Cauchy interpolation, each step of the inverse power iteration method requires solving a linear system

$$\mathcal{A}w^{(j+1)} = y^{(j)} \quad \text{with} \quad y^{(j)} = \mathcal{M}w^{(j)} \quad \text{and} \quad w^{(j)} = [v^{(j)}; u^{(j)}], \quad (28)$$

which is of the form (27). Therefore, the iterates of the inverse power method can be determined by solving

$$Su^{(j+1)} = b, \quad \text{with} \quad b = (u^{(j)} - BD^{-1}v^{(j)}), \quad (29)$$

$$Dv^{(j+1)} = (v^{(j)} - Fu^{(j+1)}). \quad (30)$$

Since D is a diagonal matrix and F is a block vector of identity matrices, $v_i^{(j+1)}$ are determined by

$$v_i^{(j+1)} = \frac{v_i^{(j)} - u^{(j+1)}}{\sigma_i}, \quad i = 0, \dots, m. \quad (31)$$

Again, exploiting the structure of D and F , the iterate $u^{(j+1)}$ can be obtained by solving (29) with

$$S = - \sum_{i=0}^m \frac{B_i}{\sigma_i}, \quad \text{and} \quad b = u^{(j)} - \sum_{i=0}^m \frac{B_i}{\sigma_i} v_i^{(j)}. \quad (32)$$

Algorithm 1 performs one step of the inverse power iteration for the Cauchy rational approximation.

Algorithm 1: One step of inverse power method for Cauchy approximation

Input : D, F, B and $C = 0$ as defined in (27),

$$w^{(j)} = \begin{bmatrix} v^{(j)} \\ u^{(j)} \end{bmatrix}$$

Output: $w^{(j+1)} = \begin{bmatrix} v^{(j+1)} \\ u^{(j+1)} \end{bmatrix}$

- 1 Compute $b = u^{(j)} - BD^{-1}v^{(j)} = u^{(j)} - \sum_{i=0}^m \frac{B_i}{\sigma_i} v_i^{(j)}$;
 - 2 Solve $Su^{(j+1)} = b$, with the Schur complement matrix $S = C - \sum_{i=0}^m \frac{B_i}{\sigma_i} = - \sum_{i=0}^m \frac{B_i}{\sigma_i}$;
 - 3 Set $v_i^{(j+1)} = \frac{v_i^{(j)} - u^{(j+1)}}{\sigma_i}$;
 - 4 **return** $v^{(j+1)}, u^{(j+1)}$
-

Inverse power iteration for the Chebyshev interpolation Recall that the iterates obtained from the inverse power method for the Chebyshev interpolation can be written as $w^{(j)} = [u^{(j)}; v^{(j)}]$. Similarly to the Cauchy rational approximation, each step of the inverse power method requires solving the linear system

$$\mathcal{A}w^{(j+1)} = y^{(j)}, \quad \text{with} \quad y^{(j)} = \mathcal{M}w^{(j)}. \quad (33)$$

Since \mathcal{M} is a block diagonal matrix, $y^{(j)} = \mathcal{M}w^{(j)}$ can be easily evaluated. The question that remains to be answered is how to solve efficiently the linear system $\mathcal{A}w^{(j+1)} = y^{(j)}$. By taking advantage of the block structure of \mathcal{A} for the Chebyshev interpolation, it follows naturally that this problem can be treated by performing the following steps, see [6, Section 2.3]. To compute the bottom part $v^{(j+1)}$ of $w^{(j+1)}$ we will use the recursion

$$v_1^{(j+1)} = y_0^{(j)}, \quad v_{2i+1}^{(j+1)} = y_{2i}^{(j)} - v_{2i-1}^{(j+1)}, \quad i = 1, 2, \dots, \quad (34)$$

for odd-numbered blocks and

$$v_0^{(j+1)} = u^{(j)}, \quad v_{2i}^{(j+1)} = y_{2i}^{(j)} - v_{2i-2}^{(j+1)}, \quad i = 1, 2, \dots \quad (35)$$

for even-numbered blocks. Since the blocks $v_{2i-2}^{(j+1)}$ in (35) are even-numbered, we can further expand the recurrence relation, i.e.,

$$v_0^{(j+1)} = u^{(j)}, \quad v_{2i}^{(j+1)} = \hat{y}_{2i-1}^{(j+1)} + (-1)^i v_0^{(j)}, \quad i = 1, 2, \dots, \quad (36)$$

where

$$\hat{y}_1^{(j+1)} = y_1^{(j)}, \quad \hat{y}_{2i+1}^{(j+1)} = y_{2i+1}^{(j)} - \hat{y}_{2i-1}^{(j+1)}, \quad i = 1, 2, \dots$$

Since $v_0 = \tau_0(z)u$ and $\tau_0 = 1$ (zeroth Chebyshev polynomial), $u^{(j+1)}$ is the top part of vector $w^{(j+1)}$, i.e., $u^{(j+1)} = v_0^{(j+1)}$ and it can be obtained by solving

$$Gu^{(j+1)} = b. \quad (37)$$

Given the number of quadrature nodes m , let us consider the Euclidean division of m by 2, i.e., $m = 2 \cdot q + r$, with quotient q and remainder r . Then the matrix G has the following form

$$G = \sum_{i=0}^q (-1)^{i+1} B_{2i}. \quad (38)$$

The vector b depends on the parity of m . If m is odd

$$b = \sum_{i=0}^{q-1} B_{2i+1} v_{2i+1}^{(j+1)} + \sum_{i=1}^q B_{2i} \hat{y}_{2i-1}^{(j+1)} + y_{m-1}^{(j)} - B_m \left(\sum_{i=0}^{q-1} (-1)^{q-i} y_{2i}^{(j)} \right), \quad (39)$$

and when it is even, then

$$b = \sum_{i=0}^{q-1} B_{2i+1} v_{2i+1}^{(j+1)} + \sum_{i=1}^{q-1} B_{2i} \hat{y}_{2i-1}^{(j+1)} + y_{m-1}^{(j)} - B_m \left(\sum_{i=0}^{q-1} (-1)^{q-i} y_{2i+1}^{(j)} \right). \quad (40)$$

Algorithm 2 implements one step of inverse power method for the Chebyshev interpolation.

To this end, only one LU factorization is required – of the Schur complement matrix S in the case of the Cauchy rational approximation or matrix G for the Chebyshev interpolation – in the preprocessing step for all q steps of the inverse power method.

Algorithm 2: One step of inverse power method for Chebyshev approximation

Input : $B_0, \dots, B_m, w^{(j)} = \begin{bmatrix} v^{(j)} \\ u^{(j)} \end{bmatrix}$

Output: $w^{(j+1)} = \begin{bmatrix} v^{(j+1)} \\ u^{(j+1)} \end{bmatrix}$

- 1 Compute $v^{(j+1)}$ using recurrences (34) and (36);
 - 2 Form matrix G defined in (38) and right-hand side vector b using (39) or (40);
 - 3 Solve linear system $Gw^{(j+1)} = b$;
 - 4 **return** $v^{(j+1)}, u^{(j+1)}$
-

Algorithm 3: Reduced subspace iteration (no restarts) for Cauchy (or Chebyshev) approximation

Input : Subspace dimension ν ; q ; Number of eigenvalues k (with $k \leq \nu$)

Output: $\lambda_1, \dots, \lambda_k, U_k$

- 1 **for** $j = 1 : \nu$ **do**
 - 2 Select $w = [v; u]$ (or $w = [u; v]$);
 /* Initially random vectors */
 - 3 Run q steps of Algorithm 1 or 2 starting with w ;
 - 4 If $w = [v; u]$ (or $w = [u; v]$) is the last iterate, then set $U(:, j) = w$;
 - 5 Use U to compute $\hat{B}_i, 0 = 1, \dots, m$ from (20);
 - 6 Solve the reduced eigenvalue problem (21) associated with (22) or (23);
 - 7 **return** $\lambda_1, \dots, \lambda_k$ and eigenvector matrix U_k
-

4. Numerical Experiments

This section will illustrate the behavior of the approaches presented in this paper for solving nonlinear eigenvalue problems in the form (5) resulting from boundary element discretization of (1) – (2). All experiments were performed with MATLAB R2018a. Furthermore, computations in Example 3 were performed in parallel on a Linux cluster at the Minnesota Supercomputer Institute that has 32 cores and 31.180 GB per-core memory.

For the presented examples, the contour Γ is either circular or elliptic and the eigenvalues of interest are those closest to the center of Γ , i.e., in Algorithms 1 and 2 the shift σ is selected to be the center of the region enclosed by the contour Γ . In the case of a circular contour, the m quadrature nodes and weights used to perform the numerical integration to approximate the functions f_j inside the contour Γ were generated using the Gauss-Legendre quadrature rule. To illustrate the effectiveness of the proposed approaches, we compare the eigenvalues obtained by each algorithm either with exact eigenvalues or the approximations obtained by the Beyn's method [19] or/and via a corresponding linearization.

no.	eigenvalue	multiplicity
1	5.441398	1
2	7.695299	3
3	9.424778	3
4	10.419484	3
5	10.882796	1
6	11.754763	6

Table 1

Approximations of the 6 smallest eigenvalues (including multiplicities) of the 3D Laplace eigenvalue problem on $\Omega = [0, 1]^3$ with homogeneous Dirichlet boundary conditions [6, Table 1].

Example 1

As our first example, we consider the 3D Laplace eigenvalue problem (1) on the unit cube $\Omega = [0, 1]^3$ with homogeneous Dirichlet boundary conditions, i.e., (2) with $a(x) = 1$ and $b(x) = 0$. The exact eigenvalues for this problem are known and given by

$$\lambda = \pi \sqrt{n_1^2 + n_2^2 + n_3^2}, \quad n_i = 1, 2, 3 \dots \dots \quad (41)$$

We are interested in the six smallest eigenvalues (including multiplicities) of (1) presented in Table 1.

To determine these eigenvalues using the Cauchy approximation technique, we will build the rational approximation of the matrix-valued function $T(\cdot)$ using circular and elliptic contours. First, we compare the accuracy between the Cauchy rational approximation and the Chebyshev interpolation of $T(\cdot)$. Note that since the eigenvalues of (1) with homogeneous Dirichlet boundary condition are real we can use the Chebyshev interpolation technique which target situations when the eigenvalues of interest lie in an interval. Figure 1 shows the errors of each approximation versus the order of approximation m for both circular and elliptic contour. For simplicity, all the errors are evaluated on a fine mesh in $[-1, 1]$, since arbitrary curves in the complex plane can be parameterized using this interval. From this figure, we can easily see that the errors in the Cauchy rational approximation and Chebyshev interpolation decay exponentially with the order of the approximation m , which implies that a moderate m is usually sufficient to reach a good accuracy. To capture the eigenvalues of interest, we first consider a circle of radius $r = 3.5$ centered at $c = 8.5$. We can then solve the linear eigenvalue problem (15) associated with (13) with $m = 25$ trapezoidal quadrature nodes by performing as many steps of shift-and-invert Arnoldi algorithm as needed to extract the 17 eigenvalues closest to the center c . The top part of Figure 2 presents the eigenvalues computed by the Cauchy approximation and those computed by the Chebyshev interpolation on a uniform mesh with 864 P1 triangular elements. Note that, in order to make a fair comparison between the two methods, the number of interpolation points for Chebyshev interpolation method is chosen to be the same as the number of quadrature nodes m . For Chebyshev interpolation method the real interval enclosing the eigenvalues of interest is chosen as [5, 12]. The bottom part of Figure 2 il-

illustrates the comparison between the accuracy of the rational approximation and the Chebyshev interpolation. The accuracy of an eigenpair (λ, u) is measured by the relative residual $\|T(\lambda)u\|_2/\|u\|_2$. Our numerical tests indicate that, to achieve a good quality of rational approximation, the quadrature nodes should be close to the eigenvalues so that they can be effectively probed. Therefore, the accuracy of the rational approximation can be considerably improved by using an elliptic contour instead of a circle. A rational approximation (10) is then built using an elliptic contour centered at $c = 8.5$ with semi-major axis $r_x = 3.5$ and semi-minor axis $r_y = 0.1$. The top part of Figure 3 presents the eigenvalues computed by the Cauchy rational approximation and those computed by the Chebyshev interpolation, and the bottom part of Figure 3 compares the relative residuals of the two methods.

We now repeat the same experiment using the Rayleigh-Ritz procedure for the Cauchy and Chebyshev approximations. To extract the 17 eigenvalues listed in Table 1, we start with a random subspace \mathcal{W} of dimension $\nu = 20$. We then apply $q = 10$ steps of inverse power method to \mathcal{W} to build a subspace of dimension ν , where each column vector is of size n . We recall that these vectors are the resulting top parts and bottom parts of the iterates of Algorithm 1 and 2 for the Cauchy and Chebyshev approximations, respectively. The resulting subspace U is then orthogonalized to obtain an orthonormal basis U that can be used to perform Rayleigh-Ritz projection that leads to a small nonlinear eigenvalue problem of size ν . This small problem is then solved by computing the eigenvalues and eigenvectors of the expanded linear eigenvalue problem (21) of size $(m + 1)\nu$. The outer iterations of the reduced procedure for the Cauchy approximation are stopped when

$$\|B_0 X f_1(\Lambda) + B_2 X f_2(\Lambda) + \dots + B_m X f_m(\Lambda)\|_F \leq tol,$$

and for the Chebyshev approximation when

$$\|B_0 X \tau_1(\Lambda) + B_2 X \tau_2(\Lambda) + \dots + B_m X \tau_m(\Lambda)\|_F \leq tol,$$

where X, Λ are the extracted eigenpairs at each iteration, $\|\cdot\|_F$ denotes the Frobenius norm and tol the desired tolerance for the convergence. In our experiments, we run as many outer iterations as needed to achieve convergence with a tolerance $tol = 10^{-12}$ for both Cauchy and Chebyshev approximations. This tolerance is achieved after 10 outer iterations for the Cauchy approximation and after 7 outer iterations for Chebyshev approximation. Furthermore, Figure 4 presents the relative residuals $\|T(\lambda)u\|_2/\|u\|_2$ for the 17 computed eigenvalues obtained using each approximation method. We emphasise that the Rayleigh-Ritz approach combined with Cauchy and Chebyshev approximations delivers more accurate eigenpair approximations than those computed by solving the linearized problem obtained directly from the Cauchy and Chebyshev approximation with projection.

Example 2

As a second example, we consider the 3D Laplace eigenvalue problem (1) on a unit sphere with homogeneous Dirichlet boundary conditions. The analytic expressions for the

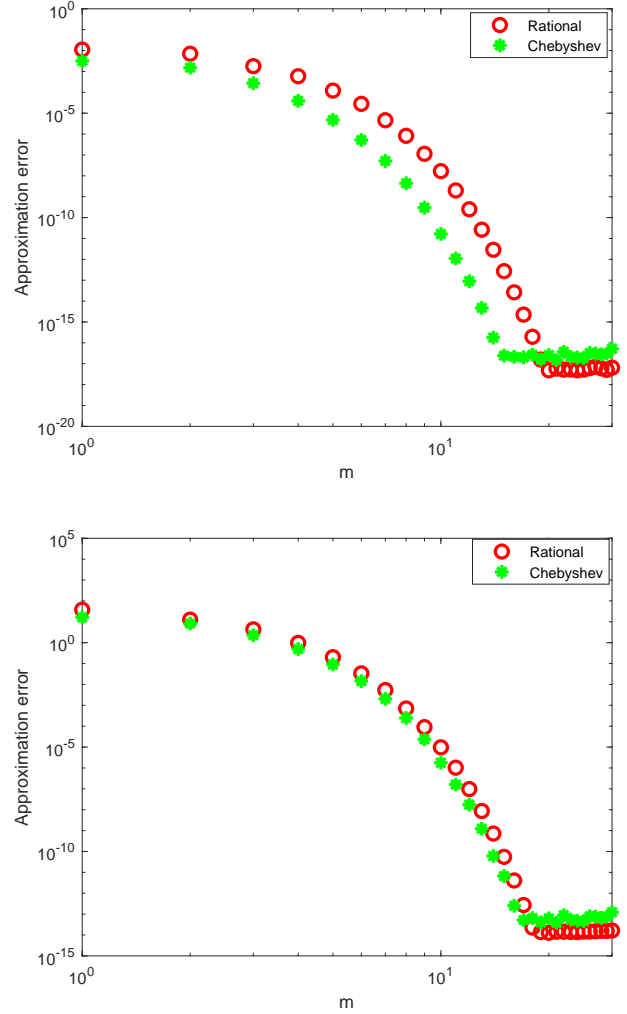


Figure 1: Top: Approximation error versus the order of the approximation m inside a unit circle. Bottom: Approximation error versus the order of the approximation m inside an ellipse centered at $c = 0$ with semi-major axis $r_x = 1$ and semi-minor axis $r_y = 0.2$.

eigenvalues for this geometry are well-known and given as the zeros of the spherical Bessel function of order ℓ . We are interested in the 6 eigenvalues of (1) listed in Table 2.

In order to compute the eigenvalues of interest using the rational approximation technique, we consider an elliptic contour centered at $c = 5.5$ with semi-major axis $r_x = 2.5$ and semi-minor axis $r_y = 0.1$. The errors of each approximation versus the order of approximation m are presented in Figure 5. The top part of Figure 6 presents the eigenvalues computed by the Cauchy rational approximation and those computed by the Chebyshev interpolation with $m = 25$ on a uniform mesh with 384 triangles, whereas the bottom part of Figure 6 illustrates the accuracy of the two methods. Also in this example, we have tested the reduced subspace iteration given by Algorithm 3. To extract the 20 eigenvalues of interest, we consider the Cauchy approximation on a circle centered at $c = 5.5$ with radius $r = 2.5$. The first outer iter-

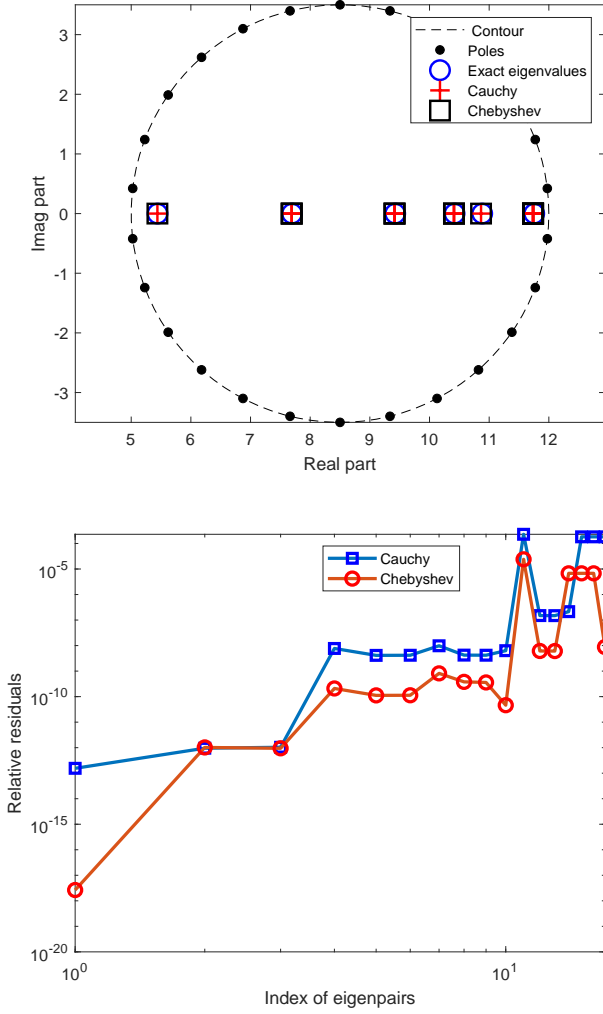


Figure 2: Top: The eigenvalues of (1) with homogeneous Dirichlet boundary conditions inside a circle centered at $c = 8.5$ with radius $r = 3.5$ (circles) computed via (15) (plus) and Chebyshev interpolation method inside the real interval $[5, 12]$ (squares). Bottom: The relative residuals $\|T(\lambda)u\|_2/\|u\|_2$ of the computed eigenpairs.

ation was carried out with a random subspace W of dimension $\nu = 25$ to which $q = 10$ steps of inverse power method, given in Algorithm 3, were applied. As for Example 1, we run as many outer iterations as needed to achieve convergence with a tolerance $tol = 10^{-12}$ for both approximation methods. Note that $q = 10$ steps of the inverse power method were applied at each outer iteration. The Cauchy approximation and Chebyshev interpolation methods achieved desired tolerance after 17 and 11 outer iterations, respectively. For completeness, we have also computed the corresponding relative residuals $\|T(\lambda)u\|_2/\|u\|_2$ for the resulting eigenpairs. These relative residuals are shown in Figure 7 for each eigenpair index.

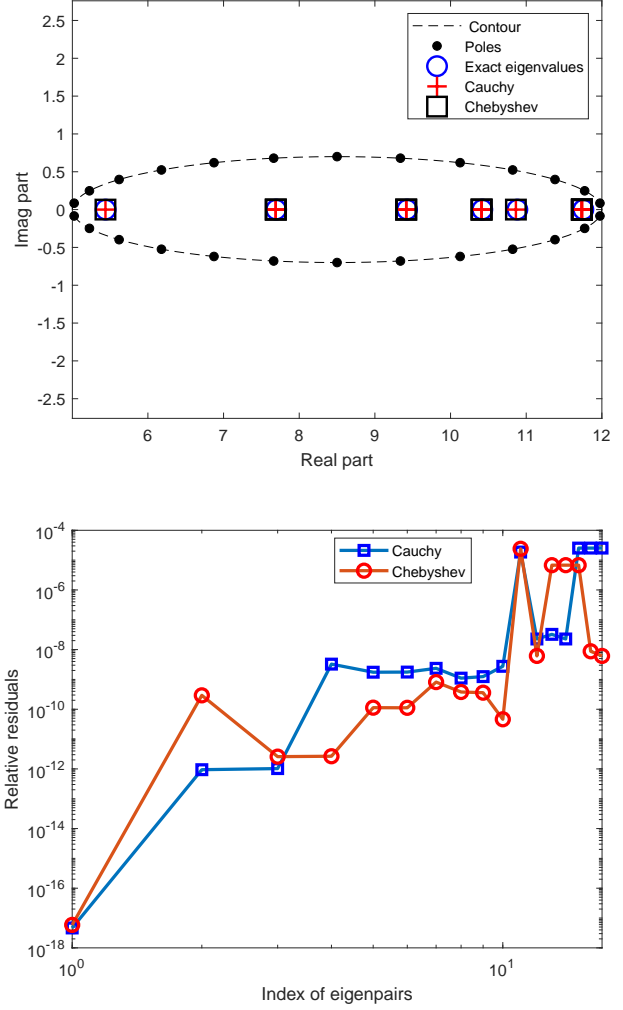


Figure 3: Top: The eigenvalues of (1) with homogeneous Dirichlet boundary conditions inside an ellipse centered at $c = 8.5$ with semi-major axis $r_x = 4.5$ and semi-minor axis $r_y = 0.2$ (circles) computed via (15) (plus) and Chebyshev interpolation method inside the real interval $[5, 12]$ (squares). Bottom: The relative residuals $\|T(\lambda)u\|_2/\|u\|_2$ of the computed eigenpairs.

Example 3

In this example, we illustrate the efficiency of the Cauchy approximation technique applied to the nonlinear eigenvalue problem resulting from BE discretization of a real-world problem of industrial relevance. We consider the geometry corresponding to a pump casing model created by using the Gmsh tool [20]. Several methods have been proposed in the literature to comprehensively study the acoustic behaviors of the pump casing [21, 22]. The boundary of the pump model displayed in Figure 8 is partitioned into 3 479 652 triangles, leading to a nonlinear eigenvalue problem with 1 728 508 DoFs. Problems of such large size add another level of difficulty to our methods, for example, we are unable to store the underlying matrices B_i in memory. To overcome this we resort to the \mathcal{H} -matrix based compression tech-

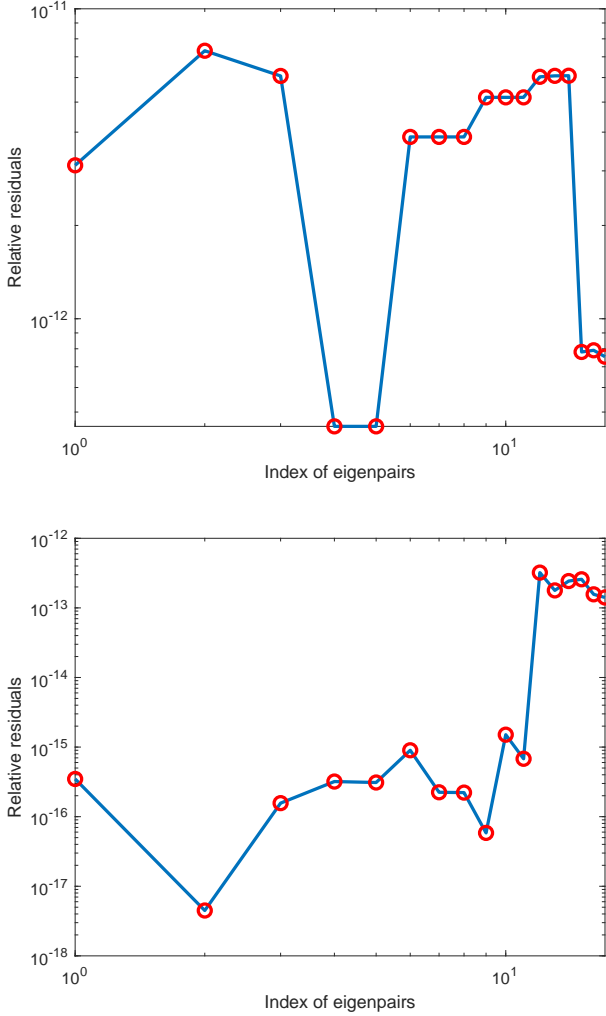


Figure 4: Relative residuals $\|T(\lambda)u\|_2/\|u\|_2$ of the 17 eigenvalues of the Laplace eigenvalue problem on the unit cube. Top: after 10 outer iterations of the reduced approach using Cauchy approximation. Bottom: after 7 outer iterations using Chebyshev approximation.

niques. Specifically, we will use the GYPSILAB toolbox library OPENHMX [23] in order to directly assemble \mathcal{H} -matrix compressed versions of matrices B_j . Here, we consider the boundary element discretization of problem (1) with a rigid boundary, i.e., $a(x) = 0$. It is well-known that application of BEM for the numerical solution of exterior Helmholtz equation may give rise to complex eigenvalues, which as we mentioned before, is the case here. In our BEM calculations, we used boundary regularized integral equation formulation of the Helmholtz equation to determine these complex eigenvalues accurately. The highly accurate results, which are of particular interest in acoustic problems of practical relevance, can be obtained by regularization of the Helmholtz kernel for example by computing a correction depending on its asymptotic behavior [24, 25]. This however also means that the fictitious solutions of the Helmholtz equation around closed surfaces are very unlikely to appear. However, it is

no.	eigenvalue	multiplicity
1	3.1416	1
2	4.4934	3
3	5.7634	5
4	6.2831	1
5	6.9879	7
6	7.7252	3

Table 2

Exact eigenvalues of the 3D Laplace eigenvalue problem on a unit sphere with homogeneous Dirichlet boundary conditions.

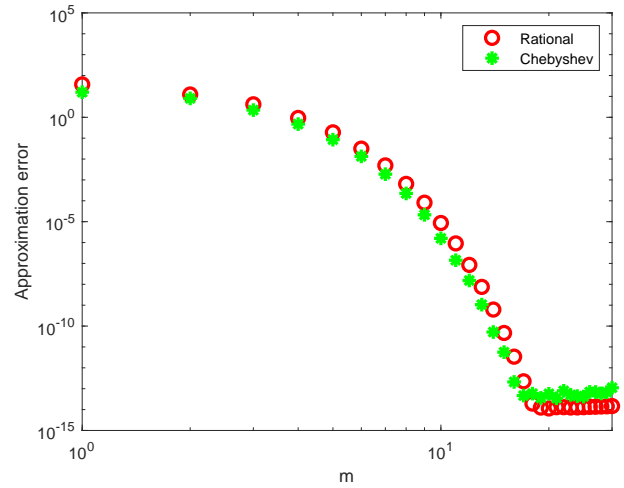


Figure 5: Approximation errors versus the order of the approximation m inside an ellipse centered at $c = 0$ with semi-major axis $r_x = 1$ and semi-minor axis $r_y = 0.2$ for the spherical BEM problem.

important to note that fictitious eigenfrequencies may occur when solving exterior acoustic BEM problems. If that is the case, the unwanted frequencies can be removed by using the Burton-Miller equation [26, 27, 28] or combined boundary integral formulation [29].

Since for this example the analytic expressions of the eigenvalues are not available, the relative residuals of the computed eigenpairs will be used to verify the accuracy of the obtained approximations.

Let the domain for the Cauchy approximation be given as a circular contour Ω centered at $c = -15i$ with radius $r = 12$. To choose a suitable order of approximation, we consider another circle Ω_1 inside Ω with the same center and radius $r_1 = r/2$ and then increase m until the resulting rational approximation inside Ω_1 is accurate enough. The eigenvalue approximations inside Ω can be obtained using a different, much coarser triangular mesh and running as many steps of Arnoldi algorithm as needed to accurately solve the expanded linear eigenvalue problem (15). We recall that only one LU factorization of the Schur complement \mathcal{H} -matrix S is required in a preprocessing step before the actual Arnoldi algorithm is invoked. In Figure 9, we present the approxima-

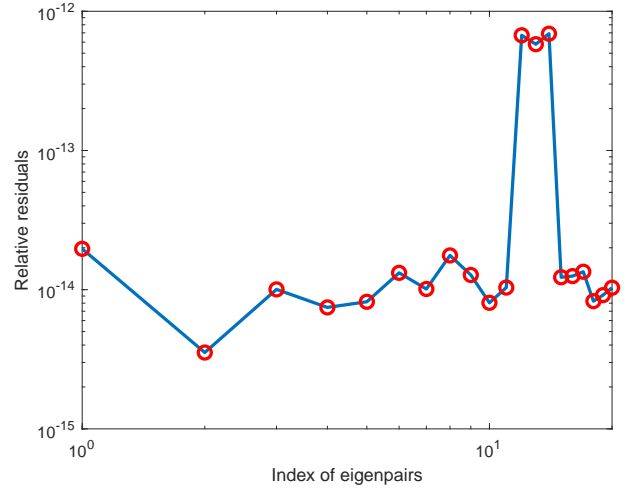
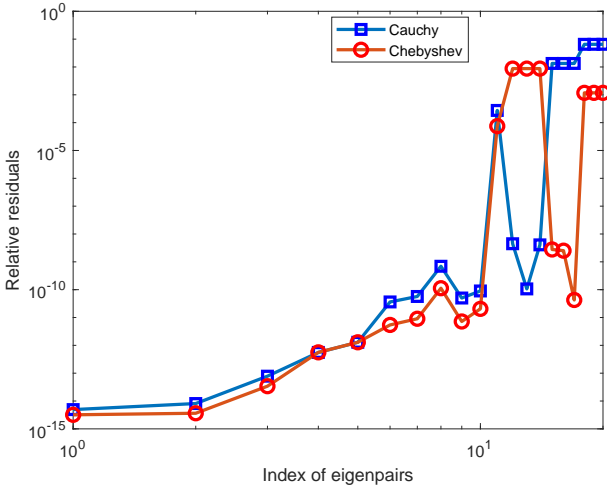
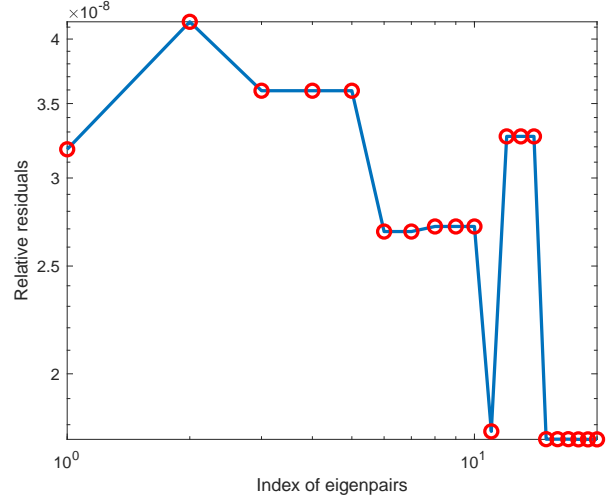
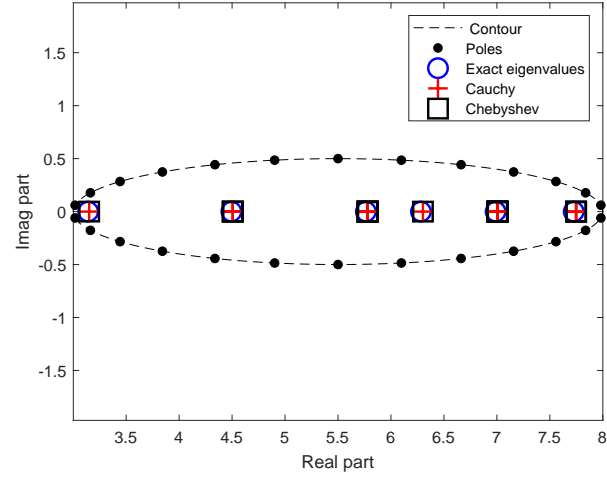


Figure 6: Top: The eigenvalues of (1) with homogeneous Dirichlet boundary conditions inside an ellipse centered at $c = 5.5$ with semi-major axis $r_x = 2.5$ and semi-minor axis $r_y = 0.2$ (circles) computed via (15) (plus) and Chebyshev interpolation method inside the real interval $[3, 8]$ (squares). Bottom: The relative residuals $\|T(\lambda)u\|_2/\|u\|_2$ associated with the computed eigenpairs.

Figure 7: Relative residuals $\|T(\lambda)u\|_2/\|u\|_2$ associated with the 20 eigenvalue approximations of the Laplace eigenvalue problem on the unit sphere. Top: after 17 outer iterations of the reduced approach using Cauchy approximation. Bottom: after 11 outer iterations using Chebyshev interpolation.

tion errors versus the order of the Cauchy approximation on a fine mesh on Ω_1 . The bottom part of Figure 9 shows that a high accuracy of the rational approximation can be reached for $m = 24$. We can therefore solve the eigenvalue problem (5) using $m = 24$ trapezoidal quadrature nodes. Forming the 24 matrices B_i and performing the matrix-vector multiplications with B_i are efficiently parallelized on 32 cores, where the per-core memory limit is ≈ 31 GB. The overall computational time is 7.3 hours. The top part of Figure 9 shows the computed eigenvalues. It turns out that there are 33 eigenvalues inside the contour Ω . The relative residuals $\|T(\lambda)u\|_2/\|u\|_2$ associated with the computed eigenvalues are presented in Figure 10 and Figure 11 shows 4 different modes of the pump model. Note that the negativity of the real parts of some of the computed eigenvalues can be related

to the existence of acoustic surface plasmon resonances [30]. These results were obtained by applying the shift-and-invert Arnoldi algorithm to solve the expanded linear eigenvalue problem obtained by Cauchy approximation on a uniform mesh with 1 728 508 P1 triangular elements.

We now consider the reduced subspace iteration approach to solve the same problem with 10704 triangles. To extract the same 33 eigenvalues displayed in the top part of Figure 9, we start with a random subspace W of size $v = 40$ and carry out 20 outer iterations of Algorithm 3 with $q = 10$ steps of inverse power method (Algorithm 1) performed at each single outer iteration. Note that Algorithm 3 is suitable for parallelization. In our tests, we have exploited parallelism for computing the matrices B_i and $\hat{B}_i = U^T B_i U$ using 32 cores. Since Algorithm 1 is applied to each vector separately to obtain a block of vectors U , the construction of the approximate subspace at each outer iteration can also be



Figure 8: Geometry and BE mesh of the pump casing model with 1 728 508 DoFs.

performed in parallel.

5. Conclusion

We have proposed two approximation methods for solving nonlinear eigenvalue problems resulting from application of boundary element method (BEM) to some types of acoustic eigenvalue problems in three dimensions. These methods are based on a newly proposed linearization which exploits the rational approximation of nonlinear functions via discretization of their Cauchy integral representation, which to our knowledge, has not been used previously. The resulting linearization fits within the broader class of so-called Block Kronecker Linearizations and therefore it inherits backward stability. One of the primary advantages of this general approach is that standard projection methods can be applied to a sequence of problems of the same size as the original problem. The rational approximation method, combined with \mathcal{H} -matrix techniques has enabled us to solve a challenging real-world problem in a boundary element approximation of 3-dimensional acoustic equations. We believe that the proposed approach can be useful in solving other classes of large scale nonlinear eigenvalue problems.

Acknowledgements

The authors would like to thank Mohammed Seaid for providing the mesh data for the test in Example 3 of the experiments and to Gmsh team for making their software available. Similarly, calculations for Example 3 in the experiments could not have been carried out without the availability of the GYPSILAB toolbox library. The authors benefitted from the hardware resources and support from the Minnesota Supercomputing Institute.

The authors thank the anonymous referees for their time, valuable comments and suggestions, which have been very helpful in improving the manuscript.

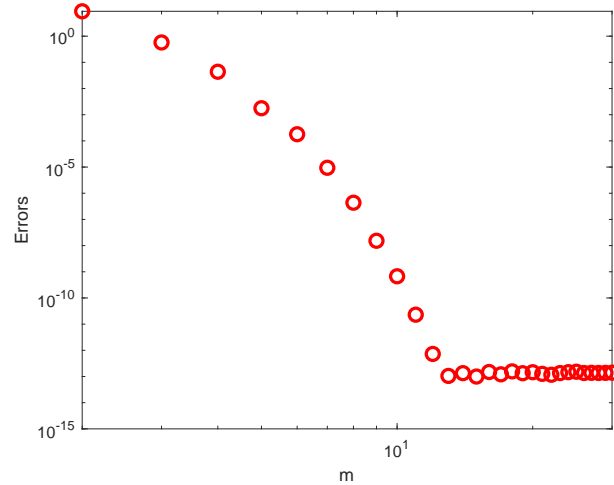
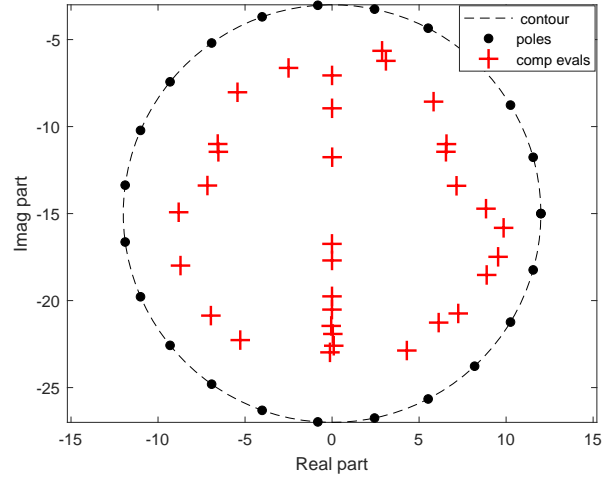


Figure 9: Top: The eigenvalues (inside a circle centered at $c = -15i$ with radius $r = 12$) of (1) on the pump model domain with Robin boundary conditions computed via (15). Bottom: Approximation errors versus the order m of the Cauchy approximation inside a unit circle.

References

- [1] S. A. Sauter and C. Schwab. *Boundary Element Methods*, volume 39 of *Springer Series in Computational Mathematics*. Springer-Verlag, Berlin, 2011. Translated and expanded from the 2004 German original.
- [2] O. Tullberg. *A Study of the Boundary Element Method in Heat Conduction, Elastostatics and Elastodynamics with Emphasis on Computer Implementation and Coupling with the Finite Element Method*. Chalmers University of Technology, 1983.
- [3] T. Sakurai and H. Sugiura. A projection method for generalized eigenvalue problems using numerical integration. In *Proceedings of the 6th Japan-China Joint Seminar on Numerical Mathematics (Tsukuba, 2002)*, volume 159, pages 119–128, 2003.
- [4] J. Xiao, C. Zhang, T.-M. Huang, and T. Sakurai. Solving large-scale nonlinear eigenvalue problems by rational interpolation and resolvent sampling based Rayleigh-Ritz method. *Internat. J. Numer. Methods Engrg.*, 110(8):776–800, 2017.
- [5] C.-J. Zheng, C.-X. Bi, C. Zhang, Y.-B. Zhang, and H.-B. Chen. Fictitious eigenfrequencies in the BEM for interior acoustic problems.

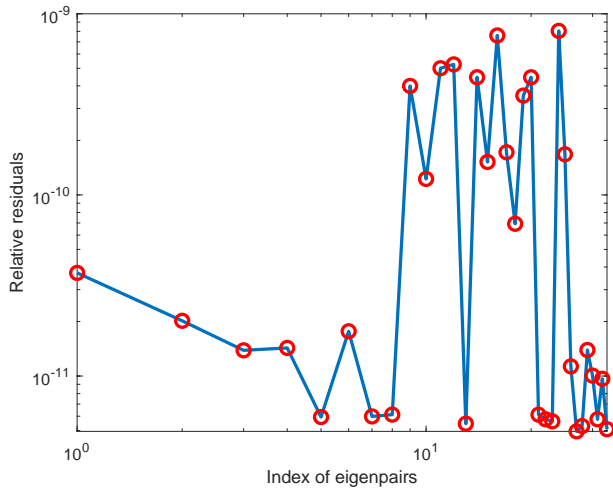


Figure 10: Relative residuals $\|T(\lambda)u\|_2/\|u\|_2$ of the eigenvalue approximations (inside a circle centered at $c = -15i$ with radius $r = 12$) of the Laplace eigenvalue problem (with Dirichlet boundary conditions) associated with the pump model displayed in Figure 8.

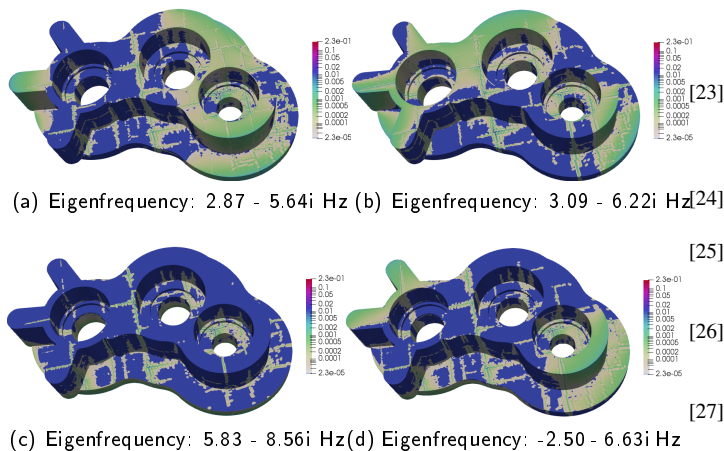


Figure 11: Eigenmodes of the pump model corresponding to four different eigenvalues

Eng. Anal. Bound. Elem., 104:170–182, 2019.

[6] C. Effenberger and D. Kressner. Chebyshev interpolation for nonlinear eigenvalue problems. *BIT*, 52(4):933–951, 2012.

[7] S. Güttel, R. Van Beeumen, K. Meerbergen, and W. Michiels. NLEIGS: a class of fully rational Krylov methods for nonlinear eigenvalue problems. *SIAM J. Sci. Comput.*, 36(6):A2842–A2864, 2014.

[8] M. Berljafa and S. Güttel. The RKFIT algorithm for nonlinear rational approximation. *SIAM J. Sci. Comput.*, 39(5):A2049–A2071, 2017.

[9] R. Van Beeumen, O. Marques, E. G. Ng, C. Yang, Z. Bai, L. Ge, O. Kononenko, Z. Li, C.-K. Ng, and L. Xiao. Computing resonant modes of accelerator cavities by solving nonlinear eigenvalue problems via rational approximation. *J. Comput. Phys.*, 374:1031–1043, 2018.

[10] P. Lietaert, J. Pérez, B. Vandereycken, and K. Meerbergen. Automatic rational approximation and linearization of nonlinear eigenvalue problems. Preprint arxiv:1801.08622. <https://arxiv.org/abs/1801.08622>.

[11] S. M. Kirkup and S. Amini. Solution of the Helmholtz eigenvalue

problem via the boundary element method. *36(2):321–330*, 1993.

[12] S. Kirkup. The boundary element method in acoustics: A survey. *Appl. Sci.*, 9(8):1642, 2019.

[13] F. Holmström. Structure-acoustic analysis using BEM/FEM; implementation in MATLAB, May 2001. Master Thesis by Structural Mechanics & Engineering Acoustics, LTH, Sweden. Printed by KFS i Lund AB, Lund, Sweden.

[14] R. D. Ciskowski and C. A. Brebbia, editors. *Boundary Element Methods in Acoustics*. Springer Netherlands, 1991.

[15] M. R. Bai. Study of acoustic resonance in enclosures using eigenanalysis based on boundary element methods. *J. Acoust. Soc. Amer.*, 91:25–29, 05 1992.

[16] Y. Saad, M. El-Guide, and A. Międlar. A rational approximation method for the nonlinear eigenvalue problem. Preprint, 2019.

[17] S. Güttel and F. Tisseur. The Nonlinear Eigenvalue Problem. *Acta Numer.*, 26:1–94, 2017.

[18] A. Amiraslani, R. M. Corless, and P. Lancaster. Linearization of matrix polynomials expressed in polynomial bases. *IMA J. Numer. Anal.*, 29(1):141–157, 2009.

[19] W. J. Beyn. An integral method for solving nonlinear eigenvalue problems. *Linear Algebra Appl.*, 436(10):3839–3863, 2012.

[20] C. Geuzaine and J.-F. Remacle. Gmsh: a three-dimensional finite element mesh generator with built-in pre- and post-processing facilities. *Internat. J. Numer. Methods Engrg.*, 79(11):1309–1331, 2009.

[21] A. Vacca and M. Guidetti. Modelling and experimental validation of external spur gear machines for fluid power applications. *Simul. Model. Pract. Theory*, 19(9):2007–2031, 2011.

[22] C. Tang, Y. S. Wang, J. H. Gao, and H. Guo. Fluid-sound coupling simulation and experimental validation for noise characteristics of a variable displacement external gear pump. *Noise Control Eng. J.*, 62(3):123–131, 2014.

[23] M. Aussal. The GYPSILAB toolbox for MATLAB version 0.5. OPENHMX library. Centre de Mathematiques Appliquees, Ecole polytechnique, route de Saclay, 91128 Palaiseau, France. www.cmap.polytechnique.fr/~aussal/gypsilab.

[24] F. Alouges and M. Aussal. FEM and BEM simulations with the gypsilab framework. *SMAI-JCM*, 4, 04 2018.

[25] Q. Sun, E. Klaseboer B.-C. Khoo, and D. Y. C. Chan. Boundary regularized integral equation formulation of the Helmholtz equation in acoustics. *R. Soc. Open Sci.*, 2.

[26] A. J. Burton and G. F. Miller. The application of integral equation methods to the numerical solution of some exterior boundary-value problems. *Proc. R. Soc. Lond. A*, (323):201–210, 1971.

[27] S. Amini and P. J. Harris. A comparison between various boundary integral formulations of the exterior acoustic problem. *Comput. Methods. Appl. Mech. Eng.*, 84(1):59–75, 1990.

[28] C.-J. Zheng, H.-B. Chen, H.-F. Gao, and L. Du. Is the Burton–Miller formulation really free of fictitious eigenfrequencies? *Eng. Anal. Bound. Elem.*, 59:43–51, 2015.

[29] O. Steinbach and G. Unger. Combined boundary integral equations for acoustic scattering-resonance problems. *Math. Methods Appl. Sci.*, 40(5):1516–1530, 2017.

[30] E. Le Ru and P. G. Etchegoin. *Principles of Surface-Enhanced Raman Spectroscopy: and related plasmonic effects*. Elsevier Science, 2008.